A fast random walk algorithm for computing diffusion-weighted NMR signals in multiscale porous media: a feasibility study for a Menger sponge

Denis S. Grebenkov, Hang Tuan Nguyen, Jing-Rebecca Li

A fast random walk algorithm for computing diffusion-weighted NMR signals in multiscale porous media: a feasibility study for a Menger sponge

Denis S. Grebenkov[1], Hang T. Nguyen[2], and Jing-Rebecca Li[3]

[1] *Laboratoire de Physique de la Matière Condensée, CNRS – Ecole Polytechnique, F-91128 Palaiseau, France*
[2] *Neurospin, CEA-Saclay, Gif-Sur-Yvette, France*
[3] *Equipe DEFI, INRIA Saclay Palaiseau, France*

Abstract

A fast random walk (FRW) algorithm is adapted to compute diffusion-weighted NMR signals in a Menger sponge which is formed by multiple channels of broadly distributed sizes and often considered as a model for soils and porous materials. The self-similar structure of a Menger sponge allows for rapid simulations that were not feasible by other numerical techniques. The role of multiple length scales onto diffusion-weighted NMR signals is investigated.

Keywords: Monte Carlo, fast random walk, restricted diffusion, confinement, PGSE, NMR, Menger sponge, fractal, self-similarity
PACS: 82.56.Lz, 02.60.Cb, 02.70.Tt, 02.70.Uu

1. Introduction

Diffusion-weighted magnetic resonance imaging (DWMRI) has became a broadly applied non-invasive experimental technique for studying the structure of natural or artificial materials (e.g., rocks, cements) and biological tissues (e.g., human organs) [1, 2]. Being inaccessible within the spatial resolution of classical MRI, the microstructure can still be revealed implicitly, through its restrictions onto diffusion of the nuclei and the resulting features of the macroscopic signal. Understanding the relation between the microstructure and the macroscopic signal is the "Holy Grail" of DWMRI, with innumerable applications in material sciences and medicine. In spite of intensive research over the last half a century, this relation remains poorly understood, especially for heterogeneous or multi-scale porous media.

From a theoretical point of view, the effect of the microstructure onto the macroscopic signal is fully described by the Bloch-Torrey equation with appropriate boundary conditions [3]. Although a numerical solution of this partial differential equation is a standard task in applied mathematics, none of the classical techniques (e.g., finite difference scheme, finite element method, Monte Carlo simulations) can be directly applied to *multi-scale* structures in three dimensions. To illustrate this point, we recall the principle of basic Monte Carlo simulations which were often applied in DWMRI [4, 5, 6, 7, 8]. For a fixed small time step δ, a random trajectory $\mathbf{r}(t)$ of restricted or obstructed diffusion at discrete times $k\delta$ is approximated by summing independent normally distributed random jumps ξ_k, with mean zero and variance $2D\delta$ along each coordinate (D being the intrinsic diffusion coefficient):

$$\mathbf{r}(k\delta) = \mathbf{r}((k-1)\delta) + \xi_k = \mathbf{r}(0) + \sum_{j=1}^{k} \xi_j$$

(the behavior near boundaries has to be treated appropriately). The total dephasing φ up to time t of an individual nucleus moving in an inhomogeneous time-dependent magnetic field $B(\mathbf{r}, t)$ is obtained by integrating the corresponding Larmor frequency $\gamma B(\mathbf{r}, t)$ along the trajectory $\mathbf{r}(t)$ and then approx-

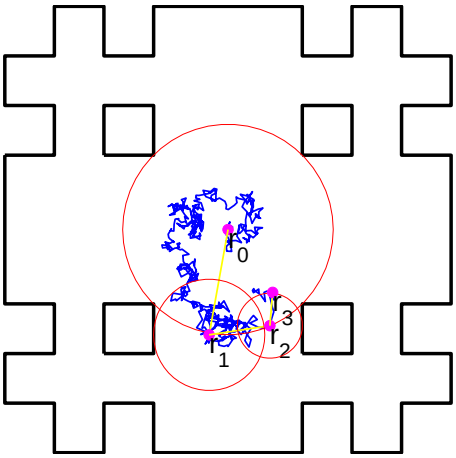

Figure 1: Illustration of the spherical process for the second iteration of a two-dimensional analog of a Menger sponge.

imated as

$$\varphi \equiv \int_0^t \gamma B(\mathbf{r}(k\delta), k\delta) \approx \delta \sum_{k=1}^{t/\delta} \gamma B(\mathbf{r}(k\delta), k\delta), \quad (1)$$

where γ is the nuclear gyromagnetic ratio. The macroscopic signal is then approximated by simulating a large number N of trajectories and the related dephasings φ_n:

$$E/E_0 = \mathbb{E}\{e^{i\varphi}\} \approx \frac{1}{N} \sum_{n=1}^{N} e^{i\varphi_n}.$$

Although these fixed-time step simulations are easy to implement, they are inefficient in hierarchical or *multiscale* porous media because the time step δ must be chosen very small in order to make the average one-step displacement $\sqrt{2D\delta}$ much smaller than the smallest geometrical feature of the domain, while most particles are released inside large pores. As a consequence, a very large number of steps (t/δ) may be required for simulating each trajectory.

2. Fast Random Walk (FRW) algorithm

This limitation was removed by Müller in 1956 by introducing the following "spherical process" [9]. From an arbitrary initial position $\mathbf{r}_0$, one draws the largest circle (or sphere in three dimensions) which is centered at $\mathbf{r}_0$ and inscribed in the confining medium (Fig. 1). Its radius ℓ_0 is the distance between $\mathbf{r}_0$ and the boundary. After diffusing inside the disk until a random time t_1, the nucleus exits the disk at a random point $\mathbf{r}_1$. Since there is no "obstacles" inside the disk, all the exit points of the disk are equally accessible for isotropic Brownian motion so that the exit point $\mathbf{r}_1$ has a uniform distribution on the circle of radius ℓ_0. The probability distribution for the exit time t_1 is known explicitly that allows one to easily generate this random variable. From $\mathbf{r}_1$, the new largest disk of radius ℓ_1 is inscribed in the confining medium. After diffusing inside the disk until a random time t_2, the nucleus exits at a random point $\mathbf{r}_2$, and so on. One thus constructs a sequence of inscribed disks (i.e., their centers $\mathbf{r}_n$ and radii ℓ_n) and the associated exit times t_n. In this algorithm, the whole random trajectory $\mathbf{r}(t)$ is replaced by a sequence of the intermediate positions $\mathbf{r}_n = \mathbf{r}(t_n)$ of the nucleus along the trajectory. This "spherical process" explores a confining medium as fast as possible because the length and time of each random jump are adapted to the local geometrical structure surrounding the nucleus (Fig. 1). Inside small pores, the nucleus moves by tiny jumps, which become much larger when the nucleus enters large pores. Making the time step δ adaptable, one removes the major drawback of basic Monte Carlo techniques. These variable-time step simulations were broadly employed by many authors, for instance, to study diffusion-reaction processes and related first-passage problems in random packs of spheres [10, 11] or near prefractal boundaries [12, 13, 14].

For DWMRI, the computation of the dephasing φ, which was elementary for basic Monte Carlo simulations with a fixed time step, now becomes a challenging problem because an approximate integration in Eq. (1) fails for variable (and potentially large) time steps. An approximate solution to this problem was recently proposed in [15]. The generated intermediate positions $\mathbf{r}_n$ (at times t_n) split the whole trajectory into pieces which are *independent* from each other due to the Markovian property of Brownian motion. Each piece of the trajectory starts from the center $\mathbf{r}_n$ of the corresponding disk at time t_n and terminates at a later time t_{n+1} at a point $\mathbf{r}_{n+1}$ on its boundary. By construction, these disks do not contain any obstacles so that one deals with a Brownian excursion inside the disk for which many statistical characteristics can be rigorously found. In particular, the random dephasing φ_n acquired by a nucleus moving inside the disk under a linear magnetic field gradient can be written

explicitly [15] from which the total dephasing φ is obtained by summing φ_n. In other words, the original problem of computing the macroscopic signal in a complex porous medium is reduced to the analysis of the dephasing in simple spherical domains. The complexity and multi-scale character of the studied porous medium enter through the generation of intermediate positions $\mathbf{r}_n$ (i.e., splitting of the trajectory), while the related dephasings are computed through explicit formulas which are only available for spherical domains. This results in a tremendous gain in computational time, as the time-consuming simulation of the dephasing φ_n inside large disks by adding tiny moves (basic Monte Carlo) is replaced by an explicit formula.

The computational efficiency of the FRW algorithm does not come for free, as this algorithm is more sophisticated than basic Monte Carlo simulations in several aspects.

(i) The construction of the intermediate positions requires a rapid estimation of the distance from any point of the medium to its boundary. In fact, this computation has to be realized for each move of each trajectory, i.e., billions of times. This problem is generic for FRWs, and many efficient solutions have been proposed, depending on the studied structure. In general, one can construct a hierarchical Whitney decomposition of the domain into boxes whose sizes are of the order of the distance to the boundary. Knowing the box in which the nucleus is currently located, one can estimate the distance. Alternatively, one can construct a set of "coarse-grained distance maps" at different length scales [12]. For some classes of domains, one can employ their specific geometrical structure (e.g., self-similarity of fractal domains or simplicity of the shape for spherical bead packings) in order to make a rapid computation [13, 14].

(ii) Although the dephasing inside each disk is determined through explicit formulas, their numerical computation should also be realized in an efficient way. This was actually the most difficult step for theoretical development in [15].

(iii) When a diffusing nucleus approaches the boundary, the moves become adaptively reduced that may significantly slow down simulations. This drawback can be removed by implementing special reflection jumps from the boundary (see [15] for details).

In order to check the feasibility and test the efficiency of the method, we apply the FRW algorithm to compute and investigate diffusion-weighted NMR signals in a Menger sponge (Fig. 2) which is formed by multiple channels of broadly distributed sizes and often used as a model for soils and porous materials [16, 17]. The self-similar structure of a Menger sponge allows one to rapidly compute the jump distances for each move. Other technical details and implementation steps of the algorithm can be found in [15].

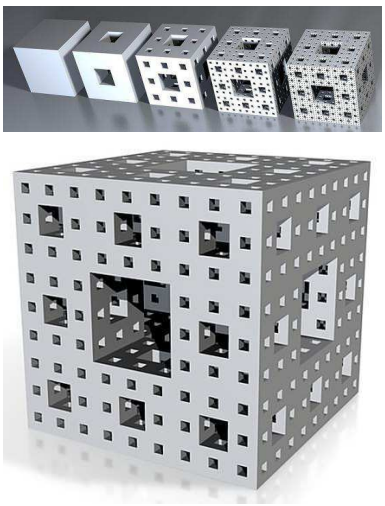

Figure 2: **(Top)** Iterative construction of a Menger sponge, by "drilling" multiple channels of various sizes. **(Bottom)**. Third level (iteration) of a Menger sponge. The nuclei diffuse inside the void region and are bounced back on the void-solid interface (Neumann boundary condition). An exterior reflecting boundary is also introduced to keep all the nuclei inside the Menger sponge (cf. Fig. 1).

3. Results and Discussion

The free induction decay (FID) at a constant gradient g is computed for levels 1-4 of a Menger sponge of size $L = 1$ (a.u.) for different times t. Figure 3a shows the absolute value of FID for levels 1-4 at a fixed time $t = 0.01$ (a.u.), computed with $D = 1$ (a.u.). The presence of multiple channels at length scales from $1/3$ to $(1/3)^4 \approx 0.012$ is reflected in different patterns of these curves. For comparison, the FID from the unit cube is shown by circles, with almost regular diffraction patterns. Figure 3b shows the absolute value of FID at times t from 10^{-4} to 10^{-1} for a fixed level 3. At short times ($t = 10^{-4}$ and $t = 10^{-3}$), the diffusion length $(2Dt)^{1/2}$ is smaller than or comparable to the width of the smallest channel $(1/3)^3 \approx 0.037$ of this domain, and the curves are close to each other. In

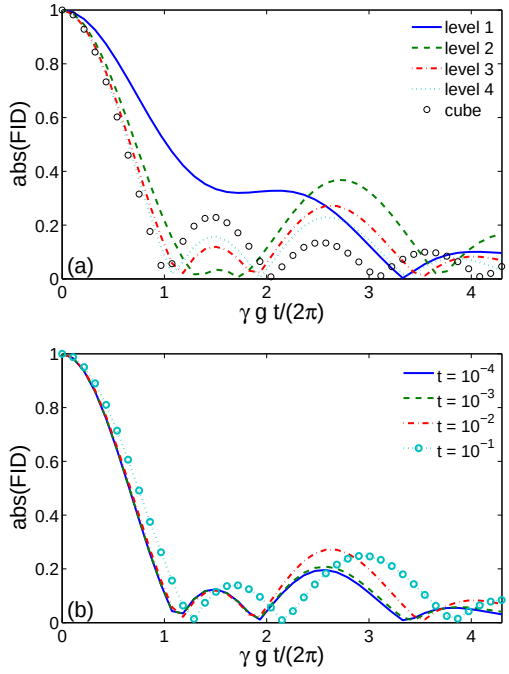

Figure 3: (Color online) Absolute value of FID as a function of $q = \gamma g t/(2\pi)$ for levels 1-4 of Menger sponge at time $t = 10^{-2}$ **(a)**, and for level 3 at different times t **(b)**. Units are fixed by setting the size L of Menger sponge and the diffusion coefficient D to 1.

turn, for $t = 10^{-2}$, the diffusion length exceeds 0.037 so that some nuclei start to "feel" the multiscale structure, yielding an increase of the third maximum. At time $t = 10^{-1}$, the diffusion length is comparable to the size of the structure, and the whole pattern is modified.

4. Conclusion

We implemented an efficient FRW algorithm for simulating diffusion in a Menger sponge. This new algorithm allowed us, for the first time, to compute and investigate diffusion-weighted NMR signals in a (model) multiscale porous medium, such a computation being unfeasible by classical (non-adaptable) numerical techniques. We showed how the FID changes when the diffusing nuclei progressively explore channels of various length scales, and revealed the role of multi-scale character of the medium onto the signal formation. These preliminary results confirmed the feasibility and efficiency of the FRW algorithm, while further analysis of diffusion-weighted NMR signals (in particular, spin-echo signals) in multiscale porous media will later be reported.

In spite of its computational efficiency, the present implementation still suffers from several limitations. First, we checked that an approximate gradient encoding suggested in [15] becomes inaccurate for short diffusion times when the nucleus performes a small number of moves. This problem can be resolved by replacing an approximate formula for the dephasing acquired within each disk by its exact expression. Its practical implementation is in progress. Second, the boundary was considered to be reflecting, while permeable frontiers in biological tissues or relaxing boundaries in mineral samples are known to play an important role for DWMRI. Their implementation presents an interesting but difficult extension from the theoretical point of view. Finally, the dephasing computation was realized only for linear magnetic field gradients. Although such encoding covers the majority of experimental setups, an extension to other spatial profiles of the magnetic field may provide a numerical scheme for studying the role of succeptibility-induced internal gradients onto multi-scale porous media.

[1] W. Price, *NMR Studies of Translational Motion*, Cambridge University Press, 2009.
[2] P. Callaghan, *Translational Dynamics and Magnetic Resonance: Principles of Pulsed Gradient Spin Echo NMR*, Oxford University Press, 2011.
[3] D. S. Grebenkov, Rev. Mod. Phys. **79** (2007) 1077-1137.
[4] B. Balinov, B. Jönsson, P. Linse, O. Söderman, J. Magn. Reson. A **104** (1993) 17-25.
[5] P. Linse, O. Söderman, J. Magn. Reson. A **116** (1995) 77-86.
[6] A. Duh, A. Mohorič, J. Stepišnik, J. Magn. Reson. **148** (2001) 257-266.
[7] R. M. E. Valckenborg, H. P. Huinink, J. J. v. d. Sande, K. Kopinga, Phys. Rev. E **65** (2002) 021306-1-8.
[8] D. S. Grebenkov, G. Guillot, B. Sapoval, J. Magn. Reson. **184** (2007) 143-156.
[9] M. E. Muller, Annals Math. Statist. **27** (1956) 569-589.
[10] L. H. Zheng, Y. C. Chiew, J. Chem. Phys. **90** (1989) 322-327.
[11] S. B. Lee, I. C. Kim, C. A. Miller, S. Torquato, Phys. Rev. B **39** (1989) 11833-11839.
[12] P. Ossadnik, Physica A **176** (1991) 454.
[13] D. S. Grebenkov, Phys. Rev. Lett. **95** (2005) 200602.
[14] D. S. Grebenkov, A. A. Lebedev, M. Filoche, B. Sapoval, Phys. Rev. E **71** (2005) 056121.
[15] D. S. Grebenkov, J. Magn. Reson. **208** (2011) 243-255.
[16] E. Perrier, M. Rieu, G. Sposito, G. de Marsily, Water Resources Res. **32** (1996) 3025-3032.
[17] C. Atzeni, G. Pia, U. Sanna, N. Spanu, Construc. Build. Mater. **22** (2008) 1607-1613.